Brazing ZrB_2-SiC ceramics to Ti6Al4V alloy with TiCu-based amorphous filler

Yaping Liu[a], Gang Wang[a,b*], Wei Cao[b], Haitao Xu[a], Zhongjia Huang[a], Dongdong Zhu[c], Caiwang Tang[d]

a School of Mechanical and Automotive Engineering, Anhui Polytechnic University, Wuhu 241000, PR China
b Nano and Molecular Systems Research Unit, University of Oulu, P.O. Box 3000, FIN-90014, Oulu, Finland
c School of Mechanical Engineering, Quzhou University, Quzhou 324000, PR China
d State Key Laboratory of Advanced Welding and Joining, Harbin Institute of Technology, Harbin 150001, PR China

Corresponding author: School of Mechanical and Automotive Engineering, Anhui Polytechnic University, Wuhu 241000, PR China
E-mail: gangwang@ahpu.edu.cn (G. Wang).

Abstract

In this work, the Ti-6Al-4V alloy and ZrB_2-SiC ultra-high temperature ceramic joint was brazed by TiCuZrNi amorphous filler at 910℃ with varied holding time. The element diffusion, microstructure and precipitation phase of the joints were analyzed in details. Reaction products in the joints were identified as β-Ti, $(Ti,Zr)_2(Cu,Ni)$, TiCu, Ti_2Cu, TiC, Ti_5Si_3, TiB and TiB_2. The formation schemes of reaction products were investigated. The holding time has substantial impacts on interfacial microstructure and shear strength of joints. A maximum shear strength of 345 MPa of the joint was reached under a brazing temperature of 910℃ and holding time of 1200 s. It is also found that the shear strength depends on the amount of eutectic structure and brittle compounds in the joints.

Keywords: ZS ceramic; TC4 alloy; Brazing; Microstructure; Shear strength

1. Introduction

As an ultra-high temperature ceramics, the ZrB_2-SiC (ZS) possesses outstanding properties such as high Young's modulus, high temperature strength and hardness, and excellent corrosion resistance [1, 2]. Thanks to these uniqueness, it has been considered as an excellent candidate for high temperature structural applications in reentry vehicles, hypersonic cruise aircraft, hypersonic flight of ballistic missiles, etc. However, constrains of its universal applications stem from difficulties to form designed shapes and/or large-sized components due to the intrinsic brittleness and inflexibility [3, 4]. To overcome the drawbacks, the ceramics has been proposed to join with other materials, especially metals and alloys. Among them, the Ti-6Al-4V (TC4) is selected as a good counterpart. This Ti alloy is widely used in aerospace industries due to its good performance [5]. In order to fully benefit two materials simultaneously, the reliable joining of TC4 to ZS is demanded.

So far, various methods have been realized to join the ceramics and metal complex [6-8]. Compared with solid phase bonding and melting welding routes, the brazing is advanced in simplicity and lower-cost natures to get robust and high quality joints of ceramic-metal. Cao *et al.* reported on a reliable brazing of ZrO_2 ceramics to the TC4 alloy using Ni-based filler foil [9]. Reliable brazing of the Si_3N_4 ceramics to the TC4 alloy was also achieved. The nano-Si_3N_4 particles were introduced into the AgCu powder filler, where the growth of continuous Ti-Cu intermetallic layers adjacent to TC4 alloy was suppressed [10]. Valenza *et al.* systematically studied the weldability and wetting of the ZrB_2/ZrB_2, ZrB_2/TC4 and ZS/TC4 using Ag-, Cu- and Ni-based filler [11-13]. The mechanism of joint formations was revealed. A satisfactory mechanical performance was obtained for ZC/TC4 joints, reaching the room temperature shear strength up to 74 MPa. Singh *et al.* showed a successful brazing of ZrB_2-based ceramic containing SiC particulates to the pure Ti

and at 1237-1257℃ with the Ni-based braze foils [14]. Furthermore, the ZS particulate ceramic-matrix composites containing either carbon powder or SCS-9a SiC fibers (79±5 μm diameter) were successfully joined to Ti and Inconel 625 using Pd-base brazes, the Palco (65Pd-35Co) and Palni (60Pd-40Ni) [15].

In spite of these progresses, however, poor wettability and mismatch of thermal expansion coefficient are two major obstacles in the welding of ceramics and metals. Consequentially, high residual stresses turn up in the joints. It is noticed that the brazing alloys, especially the reactive ones, are beneficial when brazing ceramics to metals [16, 17]. These amorphous alloys accelerate atomic diffusions, leading to reductions of residual stress in the joint. [18]. Following this scheme, the ZrB2 and SiC have been successfully brazed with the amorphous TiCuZrNi filler [19]. However, it remains unclear the feasibility to braze the ultra-high temperature ceramics to metal alloys via the similar route.

Herein, we report on brazing the ZrB_2-SiC ceramics to the TC4 alloy by using an amorphous TiCuZrNi alloy as the filler. The microstructure of joints was determined by the scanning electron microscopy (SEM) and the X-ray diffraction (XRD). The impacts of brazing parameters on the joint microstructures and mechanical properties were investigated. Based on the whole brazing process, the mechanism of joints formation was also discussed in detail.

2. Experimental

In this work, the ZS samples (SiC reinforced ZrB_2 ultra-high temperature ceramics containing 20 vol. %.) were fabricated by hot pressing. The ZrB_2 and SiC powders had a purity of 99.5% and 99%, a mean particle size of 0.7 μm and 1 μm, respectively. Prior to hot pressing, the ZrB_2 and SiC raw powders were milled in a polymer-coated bucket charged with ethanol using WC balls for 8 h

and dried in a rotating evaporator. The as-received powder mixtures were sieved through a 200 mesh and poured into a cylindrical graphite die with an inner diameter of 50 mm. BN spray was coated on graphite dies to provide smooth movement of the plunger and to avoid the direct contact of powders with graphite dies. The hot pressing was carried out at 1950 ^{o}C for 60 min in vacuum under a uniaxial pressure of 30 MPa in a graphite elements furnace. The commercially available TC4 alloy plate was employed in the present study. The $Ti_{30.21}Cu_{41.83}Zr_{19.76}Ni_{8.19}$ (at %) ingot has a melting point of 860℃. It was firstly melted in quartz tubes, and then ejected through a nozzle onto a copper wheel rotating at a velocity of 40 ms^{-1} in a purified argon atmosphere to form 30 μm thick filler foils [20]. The amorphous structure of the fabricated brazing foil was examined by an X-ray diffraction (XRD, D8, Bruker, Germany) using Cu *Kα* radiation.

The sizes of the ZS and TC4 samples for brazing were 3mm×3mm×17mm. Before joining, surfaces of the specimens were grounded and carefully polished. The filler foils were placed between the ZS and TC4 specimens to form a sandwich type, as shown in Fig.1a, and then taken into a graphite mold. The brazing process was conducted in a vacuum of 1×10^{-3} Pa. A pressure of 0.016 MPa was exerted on the brazing sample to ensure close contacts of each part, as shown in Fig.1b. At the beginning, the brazing sample was heated up to 300℃ at a rate of 10 ℃ /min and held steady for 20 min to volatilize the organic glue and clean the brazing surfaces. Then the temperature was increased to the target brazing temperature of 910℃ at a rate of 10 ℃ /min. Holding times were selected within a range of 600 s to 3000 s. Finally, the brazed samples were cooled down at a rate of 5 ℃ /min to 300 ℃, and then naturally in the furnace.

The microstructure and composition of the as-brazed samples were characterized by a scanning electron microscope (SEM, SU-8010, Hitach, Japan) with an energy-dispersive X-ray spectrometer

(EDS) for morphological and element determinations. The micro-X-ray diffraction (XRD) patterns were measured on an X-ray diffractometer (Bede D1) with Cu *Kα* at a scanning speed of 3°/min. The shear strength of the joints was measured by using an Instron 5500 testing machine at room temperature.

3. Results and discussions

Fig.2 shows interfacial microstructures and corresponding EDS results for the ZS and TC4 joint brazed at 910℃ for 1200 s. No crack is found in the joint. A complex multilayer structure, with a thickness of about 80 μm as shown in Fig.2a, appeared at the interface between the two materials. This is due to the inter-diffusion and nucleation of new phases at the brazing temperature or during cooling. Fig.2b denotes the existences of intensive diffusion between the base materials and the filler alloy during brazing process. Element distributions in the interface prove the atomic diffusion between ZS/TiCuZrNi interface and TC4/ TiCuZrNi interface. The Ti, Cu and Ni are widely distributed in the whole joint (Fig.2c, Fig.2d and Fig.2e). Due to different chemical bond types of the ZS ceramics and amorphous alloy filler, the diffusion at the ceramics-metal interface was slow. It can be seen that the Zr was mainly distributed in the ZS side of the seam, suggesting the Zr owns low diffusion rate and resides at the original location of TiCuZrNi filler foils during the brazing, as shown in Fig.2f. However, the B and Si were absent within the action layer of TC4 substrate side. This demonstrates the full reaction of the elements B and Si in the ZS side and brazing seam, as shown in Fig.2g and Fig.2i. The carbon was found in the brazed joint, as shown in Fig.2h. It migrated from the ZS composite. From Fig. 2j and Fig. 2k, the existence of V and Al in brazing beam is attributed to the dissolution and diffusion of elements from TC4 alloy into filler metal during brazing.

Fig. 3a shows detailed microstructures of ZS and TC4 brazed joint at 910℃ for 600 s. Three kinds of reaction zones were identified between the ZS ceramic and TC4 alloy. They are marked as zone I, II and III, respectively. Figs.3b-3d demonstrates the high magnification images of these three characteristic zones. In Fig. 3a, the interface between the base materials and filler alloy is rugged but without micro-cracks, denoting a well bonding. Table 1 lists the chemical compositions of the selected spots (marked as 1-5 in Fig.3b-3d) at the brazed joints through EDS. Spot 1 in Fig. 3b was mainly composed of Ti. Furthermore, a diffusion layer was formed near the TC4 side. It has been reported that Cu and Ni elements are β-Ti stabilizer elements [9, 21]. Thus, at the TC4/TiCuZrNi interfaces, α-Ti could transform into β-Ti during heating and isothermal solidification process. The black spot 2 in the zone I was mainly composed of Zr, Ti, Cu and Ni. The atom ratio of Cu+Ni and Ti+Zr is approximately 1:2. According to the Cu-Ti(Zr) binary phase diagrams, Ti(Zr)-rich liquid experiences peritectic reaction upon solidification, while eutectic solidification is found for the Ti(Zr)-rich liquid alloyed with Ni and Cu. On the other hand, both Cu and Ni are completely miscible with each other as well as Ti and Zr. Cu and Ni have a strong affinity to Ti (Zr), and they are apt to form $(Ti,Zr)_2(Cu, Ni)$. Hence, a eutectic reaction occurs during brazing process based on Cu-Ni-Ti (Zr) ternary phase diagramas $L \rightarrow \beta$-Ti + $(Ti,Zr)_2(Cu, Ni)$ [22]. According to the binary diagrams, the maximum solubilities of Cu and Ni in the β-Ti are as high as 17 at. % and 12 at. %, respectively, while they have very limited solubility in the α-Ti (1.6 at. % for Cu and 0.5 at. % for Ni) [23]. At the cooling stage, when the brazing temperature is lower than the $\beta \rightarrow \alpha$ transformation temperature, the eutectoid decomposition of β-Ti to α-Ti and $(Ti, Zr)_2(Cu, Ni)$ phases happens: β-Ti $\rightarrow \alpha$-Ti + $(Ti, Zr)_2(Cu, Ni)$. The spot 2 are considered as having a phase formula of $(Ti, Zr)_2(Cu, Ni)$, because both the elements pairs of Ti and Zr, and Cu and Ni, are not only chemically compatible

with, but also fully soluble to each other. The formation of (Ti, $Zr)_2$(Cu, Ni) phase was also demonstrated in the previous work when Ti–Zr–Ni–Cu filler metal was used [24,-26].

Fig.3c demonstrates the magnification image from zone II. The eutectic structure containing white and gray phases was formed. According to the EDS results, the white phase (spot 3) is mainly composed of Ti and Cu at an approximate ratio of 1:1. Similarly, the gray phase (spot 4) has the main contents of Ti and Cu at a ratio of 2:1. Based on the phase diagram of Ti-Cu, a eutectic reaction L→TiCu + Ti_2Cu can be observed. The TiCu/Ti_2Cu eutectic structure is formed. Fig.3d demonstrates the magnified image from zone III. For the spot 5, Si, C and Ti elements take main shares. The black spot 6 is mainly composed of B and Ti. Generally speaking, the Ti was more active than Zr [27]. Consequentially, it is easier to react with SiC during heat process, forming the Ti_5Si_3 and TiC phase. The rest Ti reacted with ZrB_2, resulting in the TiB and TiB_2 phases. From Fig.3d, the TiB phases appear as a long strip. This is due the growth velocity of TiB in [010] crystal direction is faster than other directions [28]. Figure 4 shows the micro-XRD patterns of the TC4/TiCuNiZr/ZS joint at TC4 side and ZS side, respectively. Based on micro-XRD results, chemical composition in Table 1 and phase diagrams, phases 1, 2, 3, 4, 5 and 6 can be recognized in turn as β-Ti, (Ti, $Zr)_2$(Cu, Ni), TiCu, Ti_2Cu, Ti_5Si_3 and TiC, TiB and TiB_2. However, α-Ti has not been detected by the XRD due to the small amount and the accuracy of the equipment.

From the above experimental evidences, we also proposed a possible formation mechanism of the joint and visualized it in Fig 5. Figs.5a, 5b and 5c show the interaction between filler and base metal. The TiCuZrNi amorphous filler began to melt when heated to the melting point. Then, the molten filler alloy wetted the surfaces of base materials. At the same time, partial base materials were dissolved into the molten alloy (Fig.5e). Ti_5Si_3 was firstly formed through the reaction path of

Ti + Si →Ti_5Si_3 due to the strong affinities of Ti to Si and the its lowest Gibbs free energy [29]. Similarly, the TiC was formed via the reaction of Ti + C→TiC in zone III, as shown in Fig.5f. With the temperature increase, the rest Ti in the filler further reacted with the boron in the ZS ceramic. The TiB_2 was precipitated before the TiB via the reaction of Ti + B→TiB_2 ($\Delta G \approx$ - 300 kJ/mol) due to a lower Gibbs free energy of the TiB_2 than the one of TiB [30]. Then, TiB was formed by the reactions of Ti + TiB_2→TiB in zone III, as shown in Fig.5g. However, due to the limitation of reaction time, a small amount of TiB turned out. Simultaneously, zone I was created by the diffusion of the molten alloy to the side of TC4. The products of TiCu and Ti_2Cu phases were mainly from reactions of L→ TiCu + Ti_2Cu, as shown in Fig.5h. Due to lower Gibbs free energy of the TiCu compared to the one of the Ti_2Cu in 910℃ [31], the former was ready before the precipitation of Ti_2Cu. The paths can be written as follows:

$$Ti + 1/2Cu = 1/2Ti_2Cu$$
$$\Delta G = - 17130 + 5.708T = -10377.436 \text{ J/mol}$$
$$Ti + Cu = TiCu$$
$$\Delta G = -17069 + 4.887T = -11237.679 \text{ J/mol}$$

Thus, the TiCu phase occupies a larger proportion than Ti_2Cu in zone I, as shown in Fig.3. When the solubility of Ni and Cu in Ti reached their limits, the Zr_2(Cu, Ni) and Ti_2(Cu, Ni) were produced. Meanwhile, an eutectic reaction of residual liquid phase transformed to β-Ti and (Ti, $Zr)_2$(Cu, Ni) and eutectoid decomposition of β-Ti to α-Ti and (Ti, $Zr)_2$(Cu, Ni) were under process until the solidification of the welding [32], as shown in Fig.5i.

Fig. 6 visualizes the microstructure of brazed joint with different holding time at 910℃. Three characteristic zones can be seen in all of the brazed joints, which is the same as Fig.3a. However, there are some changes in each zone following the increase of holding time. When it gets to 1200 s, the amount of the eutectic structure increased. Then, with the holding time increasing to 3000 s, the

amount of the eutectic structure decreased. However, the length of TiB and TiB_2 (as spot 5 in Fig. 3d) increased to about 20 μm as denoted in red circles of Fig.6c. Also, the diameter of TiC and Ti_5Si_3 (as spot 6 in Fig. 3d) increased to about 5 μm, as denoted in blue circles of Fig.6c. For β-Ti, the dissolved amount of TC4 was increased with holding time, leading to larger Ti element in the filler. As a result, more β-Ti phase was formed in the interface. Meanwhile, the rest Ti element would further react with ZS, forming TiC, Ti_5Si_3, TiB_2 and TiB phases between the ZS/TiCuZrNi interfaces.

Fig.7 illustrates the shear strength of TC4/ZS joints brazed at 910℃ but with different holding time. In general, samples brazed at this temperature possessed shear strength higher than 200 MPa. The strength first increased, reached the peak value of 345 MPa at 1200 s, and then decreased. When the holding time was below 1200 s, the shear strength was 254 MPa. The eutectic structure accounts for half of the joint. With the holding time increasing to 1200 s, the maximum strength achieved to about 345 MPa. Under this process, the eutectic structure occupied the entire joint. However prolongation of the holding time doesn't yield higher strength. At 1800 s, the shear strength is 262 MPa. At 3000 s, the value is 210 MPa which is lower than the one obtained at 1200 s. Such a phenomenon can be explained as follows. Under a short holding time, the amount of diffused atom was low, leading to the insufficient reaction between the filler and the base materials. But when the holding is longer, the thick interface between ZS and filler has rather big residual stress due to mismatches of the Young's modulus and the coefficients of thermal expansions between the two materials. These residual stresses induce micro-crack in the interface and deteriorate the mechanical properties [33]. On the other hand, longer holding time leads to larger amount and size of brittle intermetallics (e.g. Ti_5Si_3, TiC etc) at the interface. The formation and increases of these

intermetallics weaken the plastic deformation of the joint, which is detrimental to the relaxation of residual stress in the joint. This leads to the decrease of shear strength consequentially.

4. Conclusions

The Ti6Al4V alloy have been successfully jointed to the ZrB_2-SiC ceramics using amorphous TiCuZrNi filler and brazed at 910℃. The reaction products of β-Ti, $(Ti,Zr)_2(Cu,Ni)$, TiCu, Ti_2Cu, TiC, Ti_5Si_3, TiB and TiB_2 were detected in the brazed joint. It is found that the shear strength changes with the holding time due to the amount of eutectic structure and brittle intermetallic compounds in the joint. At 910℃ for 1200 s, a maximum shear strength of 345 MPa is achieved. Besides preparations of a high strength ceramics-metal complex, the present work is hoped to serve a brazing route for more general ceramic composites synthesis and functionalization.

Acknowledgement

This work was supported by the National Natural Science Foundation of China [grant number 51704001], Natural Science Foundation of Anhui Province [grant number 1508085SQE210], Talent Project of Anhui Province [grant number gxyqZD2016126] and the Open Fund of State Key Laboratory of Advanced Welding and Joining [grant number AWJ-16-M04].

Reference

[1] X.H. Zhang, P. Hu, J.C. Han. Structure evolution of ZrB_2–SiC during the oxidation in air. J. Mater Res, 23(2008), pp. 1961-1972.

[2] R.J. He, X.H. Zhang, P. Hu, C. Liu, W.B. Han. Aqueous gelcasting of ZrB_2-SiC ultra high temperature ceramics. Ceram Int, 38 (2012), pp. 5411-5418.

[3] P. Zhang, P. Hu, X.H. Zhang, J.C. Han, S.H. Meng. Processing and characterization of ZrB_2–SiC_W ultra-high temperature ceramics. J Alloy Compd, 472 (2009), pp. 358-362.

[4] P. Hu, Z. Wang. Flexural strength and fracture behavior of ZrB_2-SiC ultra-high temperature

ceramic composites at 1800°C. J Eur Ceram Soc, 30 (2010), pp. 1021-1026.

[5] R. Roger, E.W. Collings, G. Welsch. Materials properties handbook, titanium alloys. Materials Park, OH: ASM International; 1994.

[6] Y. Sun, J. Zhang, Y.P. Geng, K. Ikeuchi, T. Shibayanagi. Microstructure and mechanical properties of an Si_3N_4/Si_3N_4 joint brazed with Au-Ni-Pd-V filler alloy. Scr Mater, 64(5) (2011), pp. 414-417.

[7] A. Amirnasi, N. Parvin, M.Shafieihaghshenas. Dissimilar Diffusion Brazing of WC-Co to AISI 4145 steel using RBCuZn-D interlayer. J Manuf Processes, 28(2017), pp.82-93.

[8] X.R. Song, H.J. Lin, X.R. Zeng, L.L. Zhang. Brazing of C/C composites to Ti6Al4V using grapheme nano-platelets reinforced TiCuZrNi brazing alloy. Mater Lett, 183 (2016), pp.232-235

[9] J. Cao, X.G. Song, C. Li, LY. Zhao, J.C. Feng. Brazing ZrO_2 ceramic to Ti–6Al–4V alloy using NiCrSiB amorphous filler foil: Interfacial microstructure and joint properties. Mater Charact, 81 (2013), pp.85-91

[10] Y.X. Zhao, M.R. Wang, J. Cao, X.G. Song, D.Y. Tang, J.C. Feng. Brazing TC4 alloy to Si_3N_4 ceramic using nano-Si_3N_4 reinforced AgCu composite filler. Mater Des, 76 (2015), pp.40-46.

[11] F. Valenza, M.L. Muolo, A. Passerone, G. Cacciamani, C. Artini. Control of Interfacial Reactivity Between ZrB_2 and Ni-Based Brazing Alloys. J Mater Eng Perform, 21(2012), pp.660-666.

[12] F. Valenza, C. Artini, A. Passerone, M.L. Muolo, ZrB_2–SiC/Ti6Al4V joints: wettability studies using Ag- and Cu-based braze alloys. J Mater Sci 47 (2012), pp.8439-8449

[13] F. Valenza, C. Artini, A. Passerone, P. Cirillo, M.L. Muolo, Joining of ZrB_2 Ceramics to Ti6Al4V by Ni-Based Interlayers. J Mater Eng Perform, 23(2014), pp.1555-1560.

[14] M. Singh, R. Asthan. Joining of zirconium diboride-based ultra high-temperature ceramic composites using metallic glass interlayers. Mater Sci Eng A, 460-461 (2007), pp.153-162.

[15] M. Singh, R. Asthana. Joining and integration of ZrB_2-based ultra-high temperature ceramic composites using advanced brazing technology. J Mater Sci,45(2010), pp.4308-4320

[16] Y.H. Zhou, D. Liu, H.W. Niu, X.G. Song, X.D. Yang, J.C. Feng. Vacuum brazing of C/C composite to TC4 alloy using nano-Al_2O_3 strengthened AgCuTi composite filler. Mater Des, 93 (2016), pp.347–356

[17] X.R. Song, H.J. Li, V. Casalegno, M. Salvo, M. Ferraris, X.R. Zeng. Microstructure and

mechanical properties of C/C composite/Ti6Al4V joints with a Cu/TiCuZrNi composite brazing alloy. Ceram Int, 42 (2016), pp.6347–6354.

[18] W.C. Jiang, J.M. Gong, S.D. Tu, Q.S. Fan. Microstructure of high temperature Ti-based brazing alloys and wettability on SiC ceramic. Mater Des, 30(2009), pp.275–299.

[19]G. Wang, P. Xiao, Z.J. Huang, R.J. He. Brazing of ZrB_2–SiC ceramic with amorphous CuTiNiZr filler. Ceram Int, 42(2016), pp.5130–5135

[20]G. Wang, Y.J. Huang, G.C. Wang, J. Shen, Z.H. Chen. Brazing of Ti_2AlNb based alloy with amorphous Ti–Cu–Zr–Ni filler. J Wuhan Univ Technol, 30 (2015), pp.617-621.

[21] A. Cremasco, A.D. Messias, A.R. Esposito, E.A.R. Duek, R. Caram. Effects of alloying elements on the cytotoxic response of titanium alloys. Mater Sci Eng C, 31(5) (2011)), pp.833–839.

[22] Q.W Qiu, Y. Wang, Z.W. Yang, X. Hu, D.P. Wang. Microstructure and mechanical properties of TiAl alloy joints vacuum brazed with Ti–Zr–Ni–Cu brazing powder without and with Mo additive. Mater Des, 90 (2016),pp. 650–659

[23] M.K. Lee, K.H. Kim, J.G. Lee, C.K. Rhee, Growth of isothermally-solidified titanium joints using a multi-component Zr–Ti–Cu–Ni–Be amorphous alloy as a brazing filler, Mater Charact, 80 (2013),pp. 98–104.

[24]L. Li, X.Q. Li, K. Hu, S.G. Qu, C. Yang, Z.F. Li, Effects of brazing temperature and testing temperature on the microstructure and shear strength of γ-TiAl joints. Mater Sci Eng A. 634 (2015), pp.91-98.

[25]X.Q. Li, L. Li, K. Hu, S.G. Qu, Vacuum brazing of TiAl-based intermetallics with Ti–Zr–Cu–Ni–Co amorphous alloy as filler metal. Intermetallics. 57 (2015), pp.7-16.

[26]J.G. Lee, Y.H. Choi, J.K. Lee, G.J. Lee, M.K. Lee, C.K. Rhee, Low-temperature brazing of titaniumby the application of a Zr–Ti–Ni–Cu–Be bulk metallic glass (BMG) alloy as a filler. Intermetallics. 18 (2010), pp.70-73.

[27]Z.R. Li, Z.Z. Wang, G.D. Wu, J.C. Feng. Microstructure and mechanical properties of ZrB_2–SiC ultra high temperature ceramic composite joint using TiZrNiCu filler metal. Sci Technol Weld Join 16(2011), pp.697-701.

[28]H.B. Feng, Y. Zhou, D.C. Jia, Stacking faults formation mechanism of in situ synthesized TiB whiskers. Scr Mater 55 (2006), pp.667–670.

[29]T. Wang, B.G. Zhang, T. Yu, R.S. Li, X.P. Li, H.Q. Wang.. Microstructural evolution

mechanisms of Ti600 and Ni-25%Si joint brazed with Ti-Zr-Ni-Cu amorphous filler foil. J Mater Process Tech, 240 (2017), pp.414-419.

[30]Z.R. Li, X.L. Xu, Z.Z. Wang. Interfacial products of ZrB_2-SiC brazing joint and growth kinetics of reaction layer. J Mater Eng, 12(2013),pp.44-48

[31]M.F. Wu, M. Yang, C. Zhang, P. Yang. Research on the liquid phase spreading and microstructure of Ti/Cu eutectic reaction. Trans China Weld Inst, 26(10) (2005), pp.68-71

[32] Q. Qiu, Y. Wang, Z.Yang, X. Hu, D. Wang. Microstructure and mechanical properties of TiAl alloy joints vacuum brazed with Ti–Zr–Ni–Cu brazing powder without and with Mo additive. Mater Des, 90(2016), pp.650–659.

[33] X.Y. Tian, J.C. Feng, J.M. Shi, H.W. Li, L.X. Zhan, Brazing of ZrB_2-SiC-C ceramic and GH99 superalloy to form reticular seam with low residual stress. Ceram Int, 41 (2015), pp.145-153.

Figure captions

Fig.1 Illustration pictures of a) assembly and b) position of specimens during brazing

Fig.2 Interfacial microstructure and elemental distribution of ZS and TC4 joint brazed at 910℃ for 1200 s. a) BSE image and b)EDS maps of joint; c)Ti, d)Cu, e)Ni, f)Zr, g)B, h)C, i)Si, j)V, k)Al

Fig.3 (a) SEM images of the joint interface brazed at 910℃ for 600 s; (b) magnification images of zone I; (c) magnification images of zone II and (d) magnification images of zone III

Fig.4 Micro-XRD patterns of brazed joint: a) TC4 side; b) ZS side

Fig.5 Schematic of formation of each reaction layer during the brazing process: a), b) and c) show the interaction between filler and base metal; d) the filler begins to melt; e)the molten brazing alloy wetted the surface of base metals; f)the formation of Ti_5Si_3 and TiC; g) the formation of TiB and TiB_2; h) the formation of Ti_2Cu and TiCu; i) the formation of $(Ti,Zr)_2(Cu,Ni)$ and β-Ti during the cooling process

Fig. 6 Interfacial microstructure of ZS/TiCuNiZr/TC4 joint brazed at 910℃ for different holding time: a) 600 s; b) 1200 s; c) 3000 s

Fig.7 Effect of brazing parameters on shear strength of joints

Table 1 Chemical composition and possible phase of each spot marked in Fig. 2 (at. %)

Spots	Ti	Cu	Ni	Zr	B	C	Si	V	Al	Possible Phases
1	79.55	4.06	2.38	1.55	1.08	0.42	0.56	3.16	7.24	β-Ti
2	44.32	21.43	4.72	8.28	1.95	5.52	0.22	3.73	8.99	$(Ti,Zr)_2(Cu,Ni)$
3	25.72	23.24	5.09	10.71	10.31	14.02	0.57	2.70	7.17	TiCu
4	55.31	27.74	1.70	6.12	0.54	6.97	0.01	0.27	0.65	Ti_2Cu
5	43.63	13.06	1.30	2.39	3.37	20.87	10.37	1.46	3.15	$TiC+Ti_5Si_3$
6	48.10	4.52	1.56	1.85	33.53	4.56	0.25	4.67	0.66	$TiB+TiB_2$

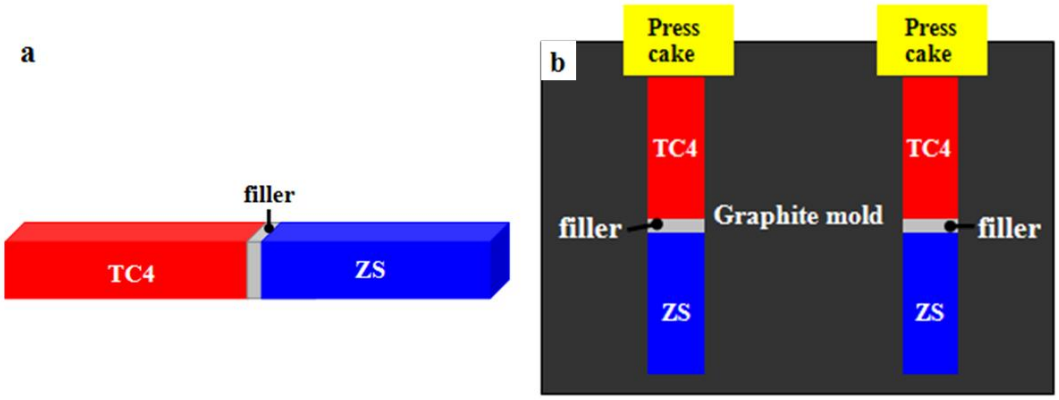
a
filler
TC4
ZS
b
Press cake
Press cake
TC4
TC4
filler
Graphite mold
filler
ZS
ZS

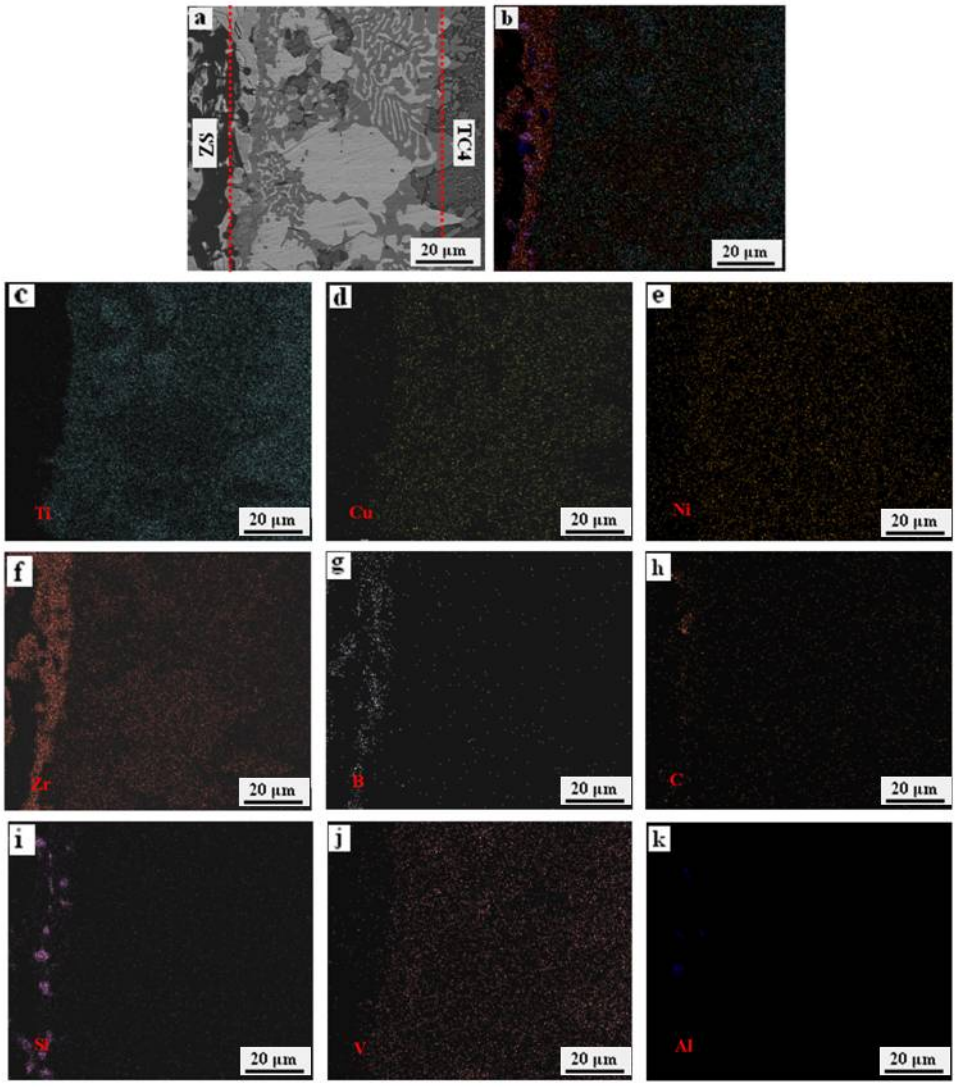
a
ZS
TC4
20 μm
b
20 μm
c
Ti
20 μm
d
Cu
20 μm
e
Ni
20 μm
f
Zr
20 μm
g
B
20 μm
h
C
20 μm
i
Si
20 μm
j
V
20 μm
k
Al
20 μm

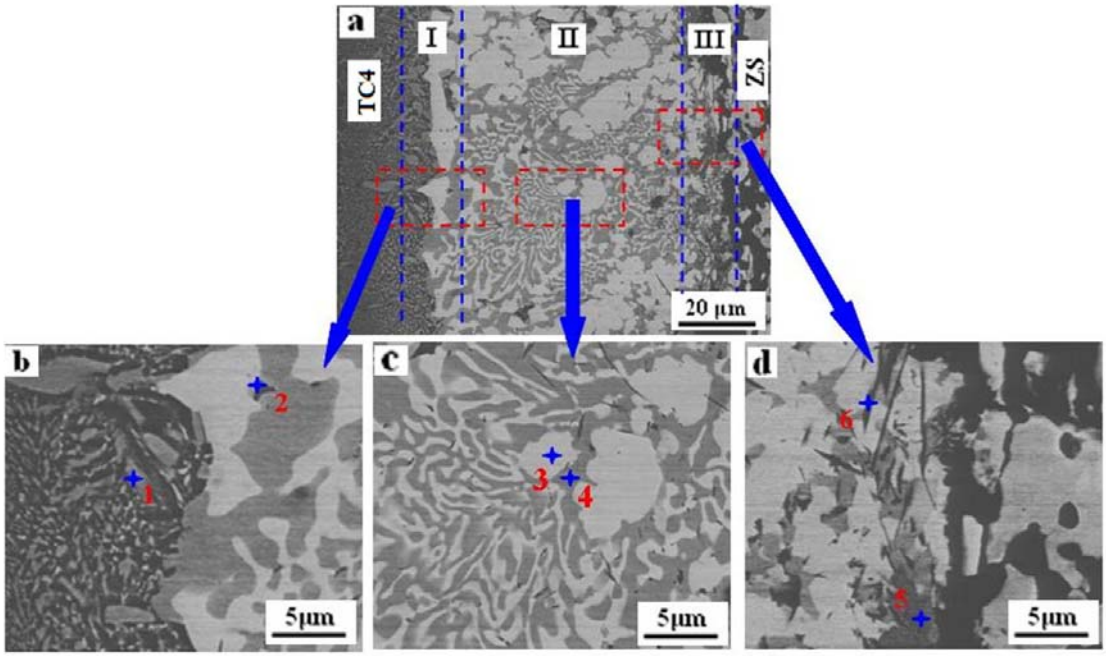
a
I
II
III
TC4
ZS
20 μm
b
c
d
1
2
3
4
5
6
5μm
5μm
5μm

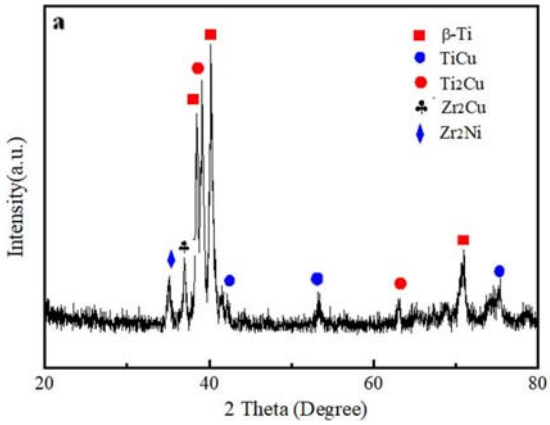
a
β-Ti
TiCu
Ti2Cu
Zr2Cu
Zr2Ni
Intensity(a.u.)
20
40
60
80
2 Theta (Degree)

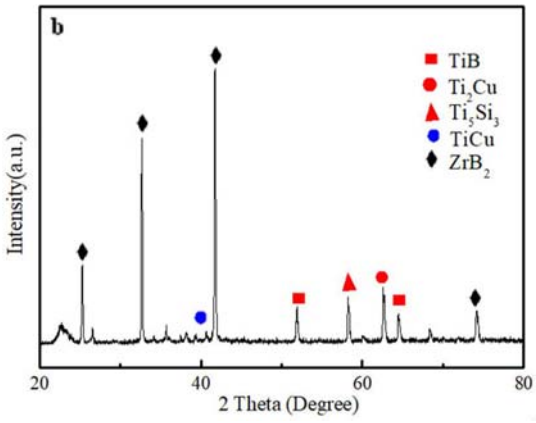
b
TiB
Ti2Cu
Ti5Si3
TiCu
ZrB2
Intensity(a.u.)
20
40
60
80
2 Theta (Degree)

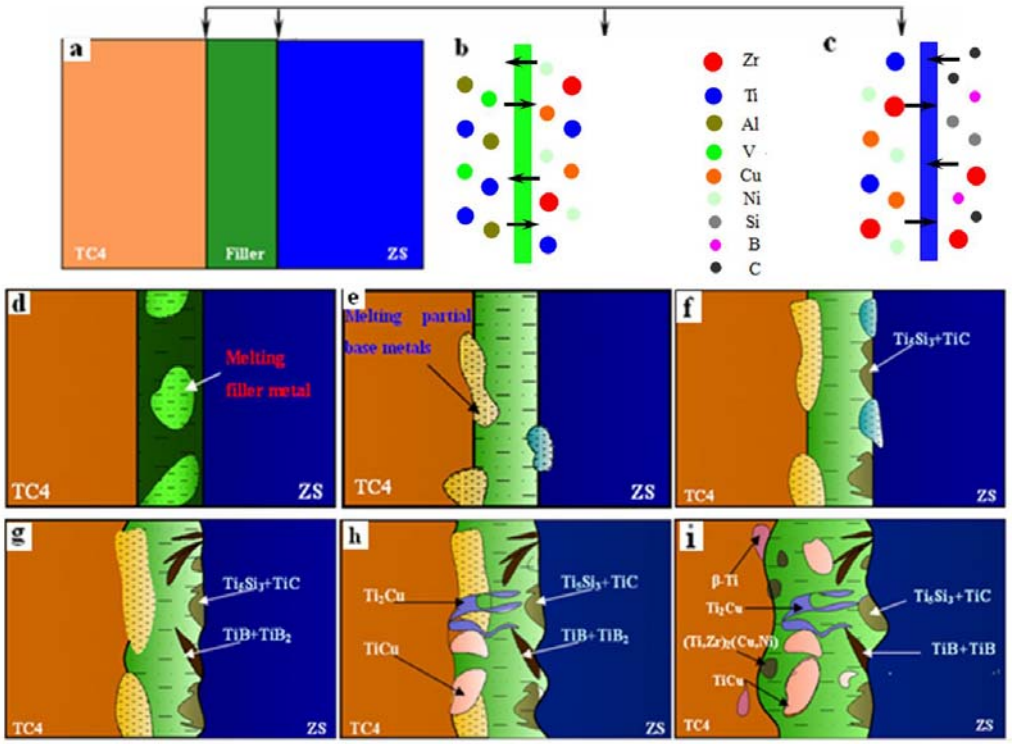
a
TC4
Filler
ZS
b
c
Zr
Ti
Al
V
Cu
Ni
Si
B
C
d
Melting
filler metal
TC4
ZS
e
Melting partial
base metals
TC4
ZS
f
Ti5Si3+TiC
TC4
ZS
g
Ti5Si3+TiC
TiB+TiB2
TC4
ZS
h
Ti2Cu
TiCu
Ti5Si3+TiC
TiB+TiB2
TC4
ZS
i
β-Ti
Ti2Cu
(Ti,Zr)x(Cu,Ni)
TiCu
Ti6Si3+TiC
TiB+TiB
TC4
ZS

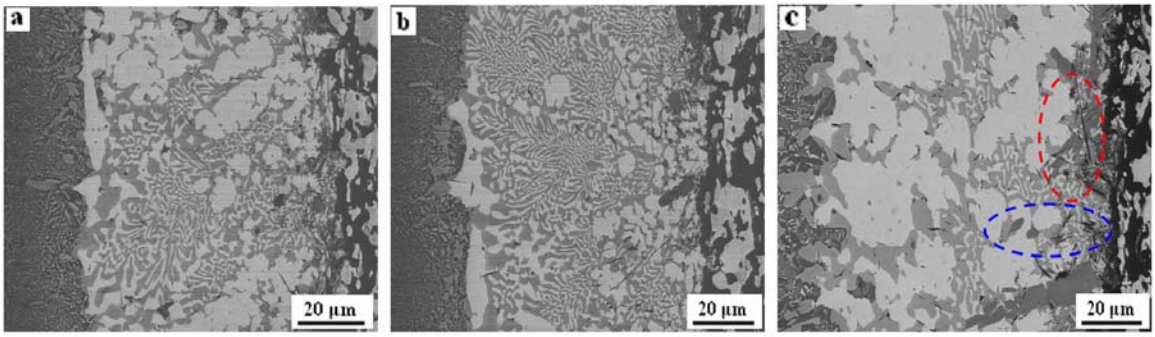
a
20 μm
b
20 μm
c
20 μm

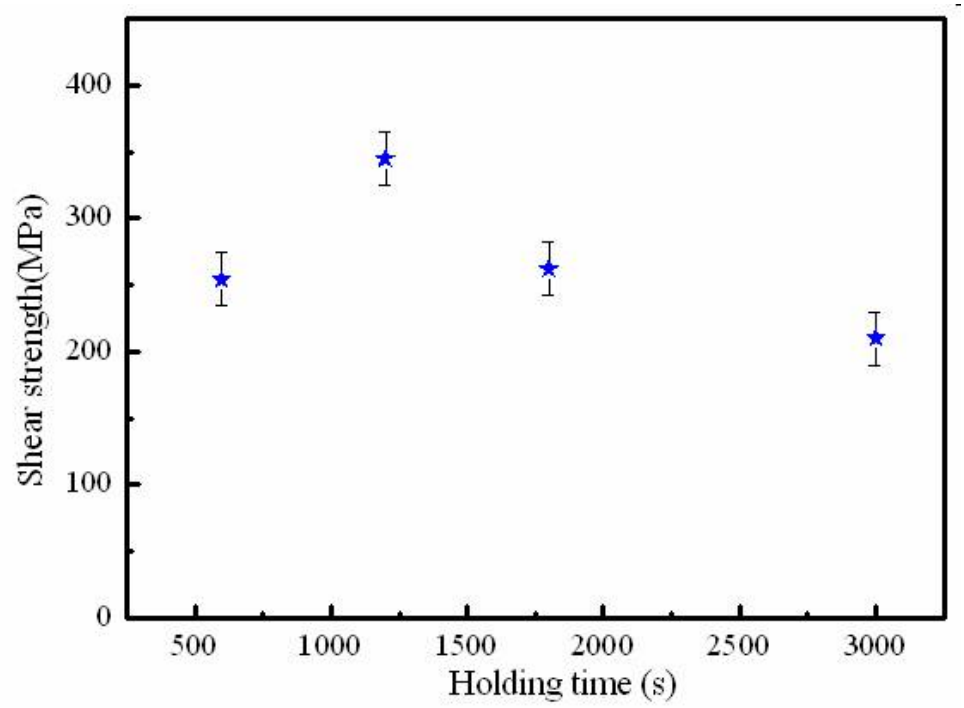
Shear strength(MPa)
400
300
200
100
0
500
1000
1500
2000
2500
3000
Holding time (s)